DTU Library

640 Gbaud NRZ-OOK data signal generation and 1.19 Tbit/s PDM-NRZ-OOK field trial transmission

Hu, Hao; Munster, P.; Palushani, Evarist; Galili, Michael; Dalgaard, Kjeld; Mulvad, Hans Christian Hansen; Jeppesen, Palle; Oxenløwe, Leif Katsuo

Published in:
OFC/NFOEC Postdeadline Papers

Publication date:
2012

Document Version
Publisher's PDF, also known as Version of record

Citation (APA):
Hu, H., Munster, P., Palushani, E., Galili, M., Dalgaard, K., Mulvad, H. C. H., Jeppesen, P., & Oxenløwe, L. K. (2012). 640 Gbaud NRZ-OOK data signal generation and 1.19 Tbit/s PDM-NRZ-OOK field trial transmission. In *OFC/NFOEC Postdeadline Papers* (pp. PDP5C.7). Optical Society of America.

640 Gbaud NRZ-OOK data signal generation and 1.19 Tbit/s PDM-NRZ-OOK field trial transmission

H. Hu[1], P. Münster[2], E. Palushani[1], M. Galili[1], K. Dalgaard[1], H.C.H. Mulvad[1], P. Jeppesen[1] and L. K. Oxenløwe[1]
[1]: DTU Fotonik, Technical University of Denmark, Building 343, DK-2800 Lyngby, Denmark
[2]: Faculty of Electrical Engineering and Communication, Brno University of Technology, Purkynova 118, 612 00 Brno, Czech Republic
huhao@fotonik.dtu.dk

Abstract: We demonstrate a field trial of a 640-Gbaud NRZ signal generated by RZ-to-NRZ conversion of a phase-coherent RZ-OTDM signal. This is employed in a 1.19-Tbit/s PDM-NRZ-OOK field transmission with BER< 3.8×10^{-3} for all 128 tributaries.

OCIS codes: (060.2330) Fiber optics communications; (070.7145) Ultrafast processing

1. Introduction

Optical networks may benefit from a combination of wavelength division multiplexing (WDM) and time division multiplexing (TDM) in terms of increasing transmission capacity and simplifying management. TDM can be realized electrically (ETDM) or optically (OTDM). Currently, the highest symbol rate and bit rate of ETDM are 100 Gbaud and 400 Gbit/s, using modulation formats of NRZ and PDM-16-QAM [1-3]. The NRZ modulation format is considered the most straightforward implementation. However, it is difficult and power hungry to further increase the symbol rate of ETDM due to the bandwidth limitation of the driving RF amplifiers. On the other hand, OTDM has achieved a symbol rate of 1.28 Tbaud and a single-channel bit rate of 9.5 Tbit/s [4-6]. However, traditional OTDM with RZ format suffers from very broad spectra making transmission very challenging.

In this paper, we report the first demonstration of a field transmission of a 640 Gbaud NRZ data signal, derived from a phase-coherent OTDM RZ signal. The 640 Gbaud NRZ OOK data signal is polarization multiplexed to a line rate of 1.28 Tbit/s, and transmitted through a 56 km field transmission link. The 640 Gbaud NRZ signal is tolerant to rectangular filtering with a bandwidth of 700 GHz with negligible power penalty. All 128 TDM tributaries (both TM and TE) are below the FEC limit after transmission, corresponding to 1.19 Tbit/s error-free field transmission.

2. Experimental setup

Fig. 1(a) shows the experimental setup for the field trial of the 1.19 Tbit/s NRZ OTDM signal. It mainly consists of a 640 Gbit/s RZ-OOK OTDM transmitter (L band), a coherent OTDM generator, a polarization multiplexer, a field transmission link, a polarization demultiplexer and a 640 Gbit/s receiver. A 640 Gbit/s OTDM RZ signal at 1590 nm is generated by optical time division multiplexing a 10 GHz short pulse, which has been on-off-keying (OOK) modulated at the 10 Gbit/s base rate with a PRBS (2^{31}-1) signal [5]. The 640 Gbit/s data pulse has a FWHM of 600 fs. To generate a phase-coherent OTDM signal, the original OTDM signal is mapped onto a coherent CW light beam. A coherent signal is needed in order to convert it to NRZ. The coherent OTDM generator is basically a polarization-rotating Kerr switch [7] as shown in Fig. 1(b). The 640 Gbit/s data pulses and coherent CW light beam at 1545 nm are launched into a highly nonlinear fiber (HNLF). At the fiber output a polarizer is placed with its axis (vertical axis in Fig. 1(b)), orthogonal to the CW light. The polarization of the data is 45° with respect to the polarizer. The 640 Gbit/s data pump switches the CW light by cross-phase modulation (XPM) induced polarization rotation in the HNLF, which generates a pulse-to-pulse phase-coherent OTDM signal. The HNLF of 128 m used in

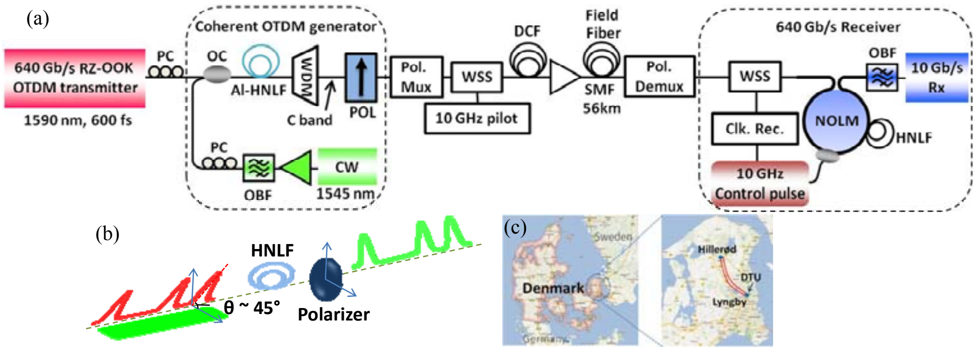

Fig. 1. (a) Experimental setup for the field transmission of a 1.28 Tbit/s Polmux-NRZ signal. PC: polarization controller, OC: optical coupler, HNLF: highly nonlinear fiber, WDM: wavelength splitter (C and L band), POL: polarizer, CW: continuous wave, OBF: optical bandpass filter, Pol. Mux: polarization multiplexer, WSS: wavelength selective switch, Pol. Demux: polarization demultiplexer, Clk. Rec.: clock recovery, NOLM: nonlinear loop mirror. (b) The principle of the Kerr switch based coherent OTDM generator. (c) Route of the field installed fiber.

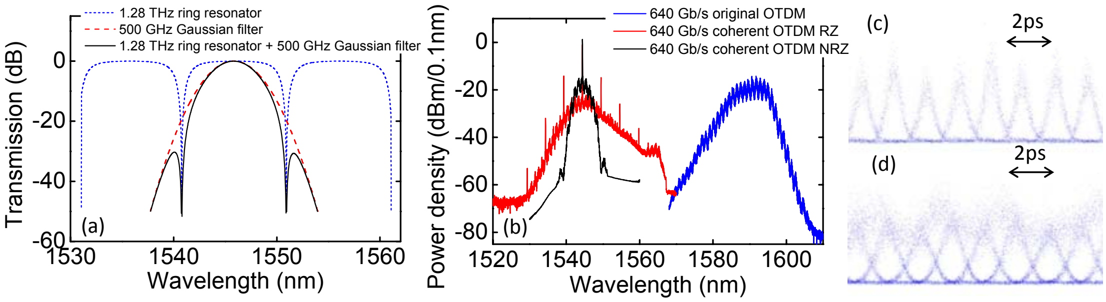

Fig. 2. (a) Filtering function of the WSS; (b) Spectra of original 640 Gbit/s L-band OTDM signal, generated 640 Gbit/s coherent OTDM RZ signal and NRZ signal; (c) and (d) optical sampling eye diagrams of the 640 Gbit/s coherent OTDM RZ signal and NRZ signal.

the experiment is alumino-silicate strained in order to increase the Stimulated Brillouin Scattering (SBS) threshold [8], and is kindly provided by OFS Fitel Denmark. The average power of the data and the CW light are 25 dBm and 27 dBm, respectively. The zero-dispersion wavelength of the Al-HNLF is at 1560 nm, minimizing the walk-off.

The 640 Gbit/s coherent OTDM signal is then polarization multiplexed by the polarization multiplexer, consisting of a polarization maintaining optical coupler, an optical delay line to provide 4800 symbol delay, and a polarization beam combiner to recombine the signal. Thus, a 1.28 Tbit/s line rate phase-coherent OTDM signal is generated, which corresponds to a data rate of 1.19 Tbit/s, after subtracting the 7% FEC overhead.

A wavelength selective switch (WSS) is used to implement a filtering function by combining those of a 1.28 THz ring resonator and a 500 GHz Gaussian filter, as shown in Fig. 2(a), in order to convert the RZ format into NRZ format. The spectra of the original 640 Gbit/s OTDM, the generated 640 Gbit/s phase-coherent RZ and the 640 Gbit/s NRZ signals are shown in Fig. 2(b). Optically sampled eye diagrams of the 640 Gbit/s coherent OTDM RZ and NRZ signals are shown in Fig.2(c-d). Finally, an in-band 10-GHz pilot tone at 1539.6 nm is inserted through the WSS for clock recovery (Fig. 3(a)).

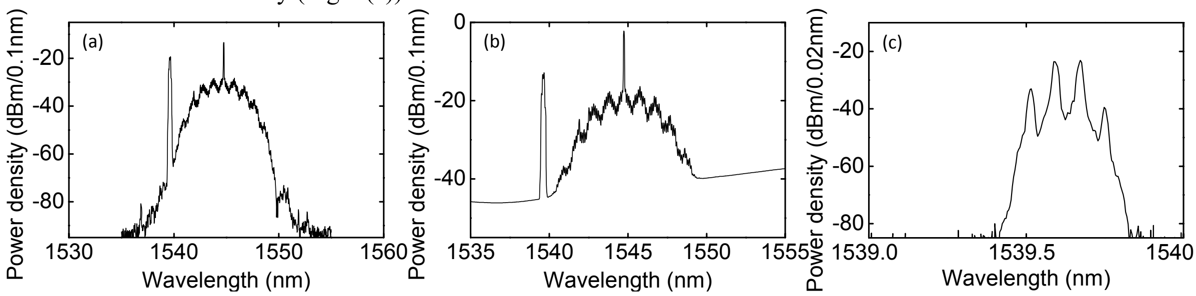

Fig. 3. Spectra of (a) 1.28 Tbit/s coherent OTDM signal with in-band 10 GHz pilot tone at the output of the transmitter; (b) 1.28 Tbit/s coherent OTDM signal with in-band 10 GHz pilot tone after the field transmission; (c) the extracted 10 GHz pilot tone in the receiver.

The 1.28 Tbit/s signal is dispersion pre-compensated by a 7-km DCF and then launched into a 56-km field transmission link, which is a loop between the DTU lab in Lyngby and Hillerød in Denmark, Fig. 1(c). The launched power into the field transmission link is 11 dBm, with less than 1 dB nonlinearity penalty when increased to 18 dBm, which is a benefit of the lower peak power of NRZ compared to RZ. The mean differential group delay (DGD) of the field installed fiber is 0.2 ps and has negligible impact on the NRZ transmission.

The spectrum of the 1.28 Tbit/s pol-MUX NRZ signal with the in-band 10 GHz pilot tone after the field transmission (Fig. 3(b)) reveals an OSNR of ~41 dB. The pol-MUX NRZ signal is then polarization demultiplexed by a polarization beam splitter (PBS) and subsequently received by a 640 Gbit/s receiver which consists of a WSS, a clock recovery (Clk. Rec.) unit, a nonlinear optical loop mirror (NOLM) based TDM demultiplexer, a 0.9 nm filter and a 10 Gbit/s pre-amplified receiver. The WSS is used to extract the 10 GHz pilot tone (Fig. 3(c)) and act as a rectangular filter with a bandwidth of ~800 GHz (tuneable) to emulate strict filtering as in a WDM system. The extracted 10 GHz clock is recovered by a phase-locked loop and then used to synchronize a mode-locked laser to generate 10 GHz control pulses. The NOLM is used to demultiplex the 640 Gbit/s data signal to the 10 Gbit/s data tributaries.

3. Experimental results

The RZ-NRZ conversion and field transmission are successful. Fig. 4 shows BER-based characterization results B2B, and Fig. 5 after the field transmission. BER vs received power is plotted for a 10 Gbit/s channel demultiplexed from the 640 Gbit/s signals. In all cases, BER values below the FEC limit are obtained. The BER performance of the optimized 640 Gbit/s NRZ signal is similar to that of the 640 Gbit/s phase coheretn RZ signal. Fig. 4(a) shows the dispersion tolerance for the 640 Gbit/s NRZ and RZ data signals. As expected, the narrower spectrum of the NRZ data leaves it more tolerant to the added β_2 dispersion than the RZ. For uncompensated dispersion of 0.2 ps/nm, the 640 Gbit/s RZ signal has an error floor at a BER of 10^{-3}, whereas the 640 Gbit/s NRZ signal just has a power penalty of 1.2 dB without an error floor. The error floor only appears for the 640 Gbit/s NRZ signal when the uncompensated dispersion is increased to 0.5 ps/nm. The 640 Gbit/s NRZ signal is also investigated for tolerance to the bandwidth of a rectangular filter, as shown in Fig. 4(b) and (c). When the filter bandwidth is larger than 700 GHz, the power penalty caused by the filtering effect is < 1 dB; however the power penalty increases dramatically when the filter bandwidth is smaller than 600 GHz.

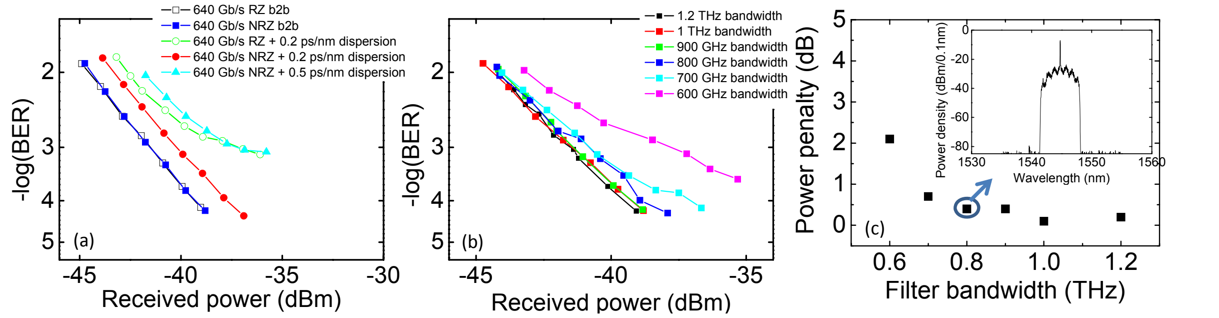

Fig. 4. B2B characterization. (a) Dispersion tolerance of 640 Gbit/s RZ and NRZ with added uncompensated dispersion. (b) Filtering bandwidth tolerance of 640 Gbit/s NRZ with rectangular filter function. (c) 640 Gbit/s NRZ power penalty at BER=3.8 × 10^{-3} for rectangular filtering with different bandwidths vs. optimum RZ case. Inset: spectrum of the 640 Gbit/s NRZ after the rectangular filtering with a bandwidth of 800 GHz.

Fig. 5(a) shows an open optical sampling eye diagram of the 640 Gbit/s NRZ signal after the field transmission. The BER performances of the 640 Gbit/s NRZ and the 1.28 Tbit/s pol-MUX NRZ signal after the field transmission are shown in Fig. 5(b). Compared to the b2b case, the power penalty of the 640 Gbit/s NRZ signal after the transmission is < 1 dB and the power penalty of the 1.28 Tbit/s pol-MUX NRZ signal after the transmission is ~1 dB for both TM and TE mode, mainly due to a limited polarization extinction ratio of the PBS in front of the receiver. The BER of all the 128 tributaries (both TM and TE) are measured with a received power of -37 dBm (Fig. 5(c)). All the tributaries of the transmitted 1.28 Tbit/s signal show a BER below 2 × 10^{-3}, well below the FEC limit of 3.8 × 10^{-3}. This corresponds to a post-FEC error-free performance (BER < 10^{-12}) at a net data rate of 1.19 Tbit/s.

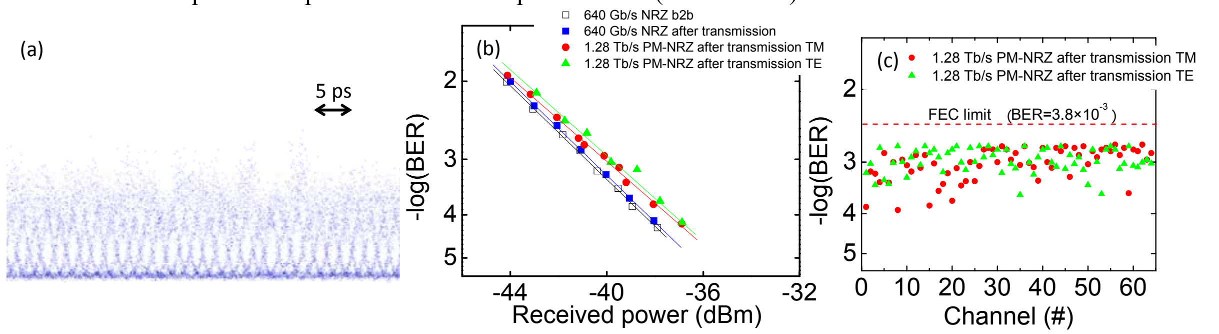

Fig. 5. Field transmission. (a) Optical sampling eye diagram of the 640 Gbit/s NRZ signal after the field transmission. (b) BER measurements for 640 Gbit/s NRZ back-to-back, 640 Gbit/s NRZ after field transmission, and for 1.28 Tbit/s pol-MUX NRZ after field transmission (TM and TE). (c) BER measurements for all the 128 tributaries (TM and TE) at a receiver power of -37 dBm.

4. Conclusion

We have demonstrated the generation of a 640 Gbaud NRZ signal and a field trial of a 1.19 Tbit/s PDM-NRZ-OOK signal over a 56 km installed transmission link. All 128 tributaries show a BER below the FEC limit of 3.8×10^{-3} after the field transmission. The bandwidth of the generated 640 Gbaud NRZ signal can be restricted to 700 GHz with negligible power penalty. Furthermore, the phase coherent OTDM NRZ signal with narrower spectrum has better tolerance to dispersion compared to a traditional OTDM RZ signal.

5. Acknowledgements

We would like to acknowledge GlobalConnect A/S (Denmark) and UNI-C for supporting the field transmission link and OFS Fitel Denmark for providing the Al-HNLF.

6. References

[1] G. Raybon et al., OFC 2006, PDP 32.
[2] R. H. Derksen et al., OFC 2006, PDP 37.
[3] P. J. Winzer et al., ECOC 2010, PD 2.2.
[4] H. C. Hansen Mulvad et al., Opt. Express, 18, pp. 1438, 2010.
[5] P. Guan et al., Opt.Express 19, pp. B567-B573, 2011.
[6] T. Richter et al., OFC 2011, PDPA9.
[7] Y. Ding et al., Opt. Express, 19, pp. 6471, 2011.
[8] L. Gruner-Nielsen et al., ECOC 2010, Tu.4.D.3.